XVII IMEKO World Congress
Metrology in the 3rd Millennium
June 22–27, 2003, Dubrovnik, Croatia

EXPERIMENTAL ULTRASONIC FLOW MEASUREMENT IN SMALL CAPILLARIES

Florian Maier, Bernhard G. Zagar

Institute for Measurement Technology, Johannes Kepler University of Linz, 4040 Linz, Austria

Abstract – In this paper we present preliminary results of an ultrasonic flow measurement set-up designed to accurately measure the flow velocity profile of blood mimicking fluid pumped through a capillary flow phantom even under the deteriorating effects of clutter and noise always seen in medical ultrasound applications. The measurement system is set up in a way to acquire and display 3-dimensional velocity and/or topological data.

Keywords flow measurement ultrasonic

1. INTRODUCTION

Ultrasonic scanning systems due to their non-invasive and non radiative properties are very wide spread in medical imaging. Recent developments [2] have shown that ultrasonic interrogation of tissue allows to detect deviations of normal vascularization indicative of malignant processes for example in breast tissue. This is done by detecting small to very small blood vessels and determining their 3-dimensional structure were in case of malignancy for example arterial loops can form.

Furthermore vascular disease, a very wide spread condition can be detected fairly early on if flow profiles with high spatial, temporal and flow velocity resolution can be measured.

Modern standard medical equipment utilizes ultrasound frequencies in the range of 2 MHz up to 10 MHz thus allowing a typical spatial resolution approximately by the wavelength λ of 770µm down to 150µm. In order to accommodate the even higher spatial resolution sought frequencies on the order of 35MHz are necessary.

We report preliminary results of a signal acquisition and processing framework for an experimental set-up which is designed to also cope with vibrations always expected with living tissues due to heart action, respiration and tremor always seen in subjects.

2. EXPERIMENTAL SET-UP

Since our goal is to develop an automated 3-dimensional ultrasonic scanning system we initially constructed the mechanical as well as the electrical components as they are depicted in Fig. 1. Furthermore the associated schematics is shown in Fig. 2.

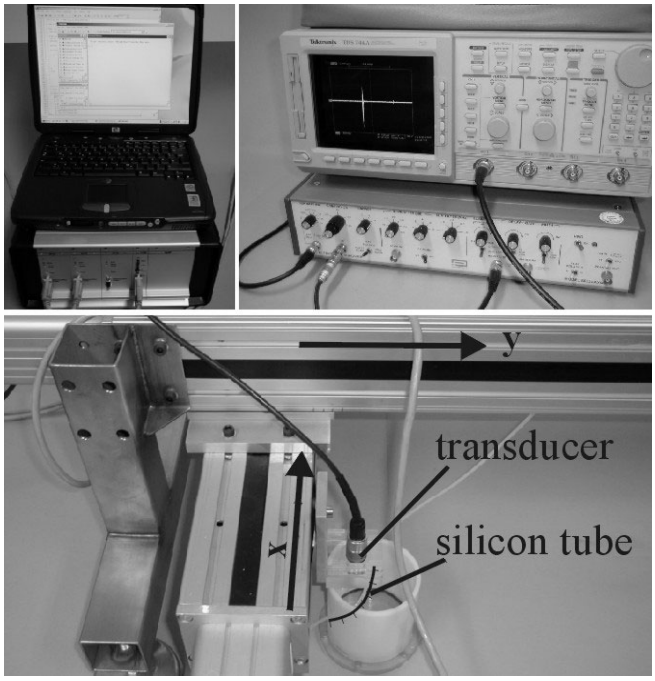

Fig. 1. Shows the experimental set-up of a 3-dimensional ultrasound scanner. Upper left shows the PC and the translation stage controller, in the upper right photo the TDS 744 scope and the pulser/receiver are shown, lower part shows the phantom in a water bath and the transducer stage.

It consists of a PC running MATLAB depicted in Fig. 1 upper left, a panametrics ultrasonic analyzer model 5052UA capable of pulse repetition rates between 100Hz and up to 5kHz, with pulse voltages of up to 300V and rise times of 10ns (10% to 90%) with no external load, a Tektronix scope used as transient recorder depicted in Fig. 1 upper right, and a panametrics transducer mounted onto a translation stage depicted in Fig. 1 lower part.

The transducer output is fed into the ultrasonic analyzer (gain 40dB ± 1dB, 50MHz bandwidth) increasing the return amplitude to levels easily handled by the attached Tektronix TDS 744A digitizing oscilloscope with 500MHz bandwidth and 8bit quantization. The 500k words memory record length of the scope allows to record in a single shot data for each line of sight (LOS) up to more then n_p =100 consecutive pulses digitized with a maximum sampling rate of 2G samples/s. For each recorded pulse (index j) m samples ($m \cdot n_p \leq$ 500k words) are stored. The transducer type panametrics A309R has a spherical face plate with

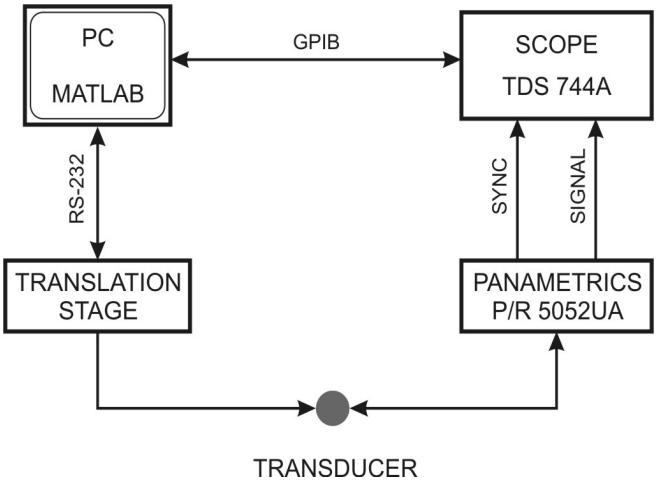

Fig. 2. Schematics of the experimental set-up shown in Fig. 1.

50.8mm focal length and a 5MHz center frequency. It is moved in 2 dimensions by a PC controlled translation stage (Isel C-10 controller with two linear units) with an accuracy better than 125μm. Thus allowing to accurately position the transducer on a regular grid which is necessary later in the reconstruction part.

The flow phantom consists of silicon tubing with an inner diameter of 1.75mm and a wall thickness of 0.75mm. It is fed by a pump to maintain a stationary controllable flow of a blood mimicking water, glycerol and nylon particles mixture. The blood cells are simulated experimentally through a mixture of water and plastic powder brand name: VETOSINT.

For experimental purposes it is necessary to scale up our system and the phantom parameters (mainly its geometry) to simulate blood flow within arteries down to approximately 0.25mm in diameter. To accommodate the current 5MHz transducer plastic powder with an average diameter of approximately 90μm was used which fits nicely to red blood cells if a scaling factor K of 7 is assumed thus simulating the sought 35MHz transducer center frequency. The particle size was determined by a scanning electron microscope. The scaling factor K as shown in (1) determines a wide range of parameters to keep the flow at equivalent Reynold numbers if Newtonian fluid could be assumed which is not the case. Table I shows the comparable parameters between blood and water.

TABLE I. Comparable parameters

	Water	Blood
Inner tube diameter	D_S=1.75mm	D_B=0.25mm
Transducer center frequency	f_{0S}=5MHz	f_{0B}=35MHz
Wavelength	λ_S=300μm	λ_B= 42.9μm
Particle size	d_S=90μm	d_B=13μm
Viscosity	μ_S=0.001kg/m·s	μ_B=0.004kg/m·s
Velocity range by R_e<1000 (laminar flow)	0 ... 0.57m/s	non Newtonian

$$K = \frac{f_{0B}}{f_{0S}} = \frac{\lambda_S}{\lambda_B} = 7 \quad (1)$$

The Reynolds number (2) gives a rough indication of whether the flow will be turbulent or laminar.

$$R_e = \frac{2 \cdot R \cdot \rho}{\mu} \cdot \overline{v} \quad (2)$$

The parameters in (2) are: the inner radius, R, the fluid density, ρ, is dynamic viscosity, μ, and $\overline{v}$ the spatial averaged velocity within the tubing. In our calculation we choose Reynolds numbers less then 1000 indicative of laminar flow. The Reynolds numbers are comparable if the fluid flowing through the tubing has a viscosity μ_{water}=0.001kg/(m·s) as compared to blood with μ_{water}=0.004kg/(m·s). The mean density of the blood cell mimicking particles is 1060kg/m^3. The speed of sound, c, is assumed for both systems to be 1540m/s.

A depiction of the flow phantom cube is seen in Fig. 3. It shows a cubic box with an edge length of 20mm which is scanned slice by slice beginning from y=0mm up to y=20mm in 0.5mm increments. Slice planes are indexed by k and the plane with k=10 is indicated by the dashed line referring to results presented later on. In each slice plane data for 81 lines of sight (LOS shown in bold in Fig. 3) is acquired thus giving a spatial resolution within the plane of 250μm. The transducer is positioned 40mm above this box so as to focus the pulse at approximately the middle of the current LOS.

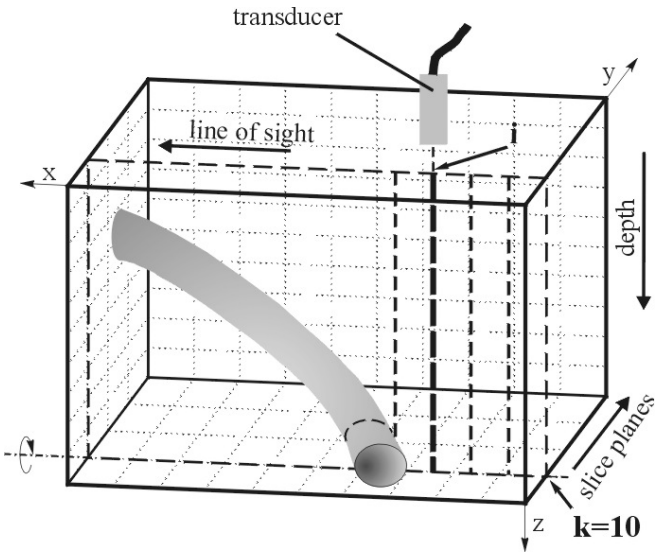

Fig. 3. This schematic shows the employed flow phantom, a flexible tube within the scanned volume indicated by the box with an edge length of 20mm. The current LOS (index i) in slice plane k=10 is shown by the bold dashed line extending in z direction.

3. SIGNAL PROCESSING

Since scattering of blood is still approximately 27dB down at transducers frequencies of 35MHz with respect to returns from vessel walls wall filtering action has to be

provided by the signal processing algorithm to enhance low returns from blood.

3.1 Alignment

Effective wall filtering action can only be performed if all presumed stationary targets also cause stationary returns. Fig. 4 shows typical M-mode (motion mode) image of raw data were one can see the dramatic deteriorating effect of all sort of subjects motions like heart action, respiration and tremor. On the left hand side the raw data is shown on the right hand side the so-called alignment procedure had been performed to make the data suitable for subsequent wall filtering. One can also see rather weak signal components due to flow in between the inner and the outer wall not discernable in the left image.

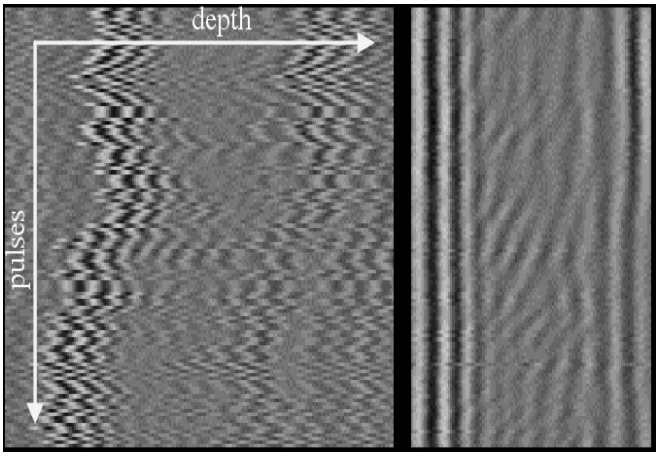

Fig. 4. Shows a typical M-mode image left: raw data, right: after proper alignment (slanted structures constitute flow)

Since as far as this paper is concerned phantom data is processed currently no prealignment is done before velocity estimation.

3.2 Wall filtering

We model the digitized transducer signal *r(n)* as shown in (3). *s(n)* is the discrete time transducer signal sent into the volume, *j*, is the pulse index, *m*, is the total number of recorded samples per pulse (*m* is 5000 in our case), *z(t)* is a time dependent depth of any scatterer pointing away from the transducer, *c*, is the speed of sound, *N(n)* is a noise term and *C(n)* a typically dominant clutter term that needs to be suppressed by wall filtering. $\lfloor \ldots \rfloor$ represents the floor operator, thus evaluating the scatterers depth to a discrete time round trip delay.

$$r(n) = A \cdot \sum_{j=o}^{j_{\max}} s\left(n - j \cdot m - \left\lfloor \frac{2z(t)}{c} \right\rfloor\right) + N(n) + C(n) \qquad (3)$$

By rearranging terms to get a two dimensional signal *r´(j,l)* out of the only time (index *n*) dependent signal *r(n)* the wall filtering action is much easier to comprehend (4).

$$r'(j,l) = r(j \cdot m + l) \qquad \begin{matrix} j = 0,1,2,\ldots, j_{\max} - 1, \\ l = 0,1,2,\ldots, m-1 \end{matrix} \qquad (4)$$

In (4) the parameter *j* is the index running over all pulses up to j_{max} which in our case was 15 and *l* is the index representing samples within a single pulse. The result of rearranging is the so called M-mode image an example of which is shown in Fig. 5 left image. The wall filter represented by its impulse response *h(j)* is applied by convolving the columns of *r´(j,l)* with *h(j)*

$$r''(j,l) = r'(j,l) \otimes h(j) \qquad (5)$$

where $\otimes$ means column wise convolution. *h(j)* is actually implemented through a 6th order step initialized Bessel high pass filter with a relative cutoff frequency of 0.1. The wall filter efficacy is demonstrated in Fig. 5 right hand side

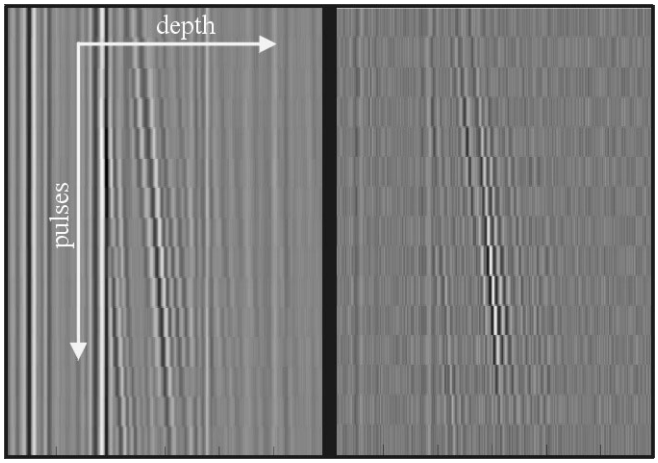

Fig. 5. Wall filtering action on an M-mode image. Input *r´(j,l)* shown left, output *r´´(j,l)* shown right

were one can see the filtered data as compared to the left image where the aligned raw data is shown. The stationary clutter component is fairly well suppressed and the flow component represented by the slanted structures is preserved. The data in Fig. 5 consists of 15 pulses acquired for a single line of sight.

3.3 Velocity estimator

Subsequent to signal alignment and wall filtering action the velocity estimation is performed. A tradeoff between processing speed and accuracy is made. For a preliminary interrogation of a volume a fast cross correlation based algorithm was chosen [1].

The signal *r´´(j,l)* consists of $\lfloor m/N_s \rfloor$ adjacent segments of size j_{max} times N_s, the index i_{seg} is essentially specifying a depth window.

The position of the correlation maximum is indicated by n_{max} and can be calculated by locating the maxima position of $\hat{R}_{12}$ in (7) so that each segment is associated with a velocity

$$v_z(i_{seg}) = \frac{c \cdot f_{prf}}{2 \cdot f_s} \cdot n_{\max}(i_{seg}) \,. \qquad (6)$$

In (6) f_{prf} is pulse repetition frequency, f_s, is the sampling frequency and c, is the speed of sound.

The discrete time cross-correlation estimate $\hat{R}_{12}$ is calculated by:

$$\hat{R}_{12}(n_{\max}, i_{seg}) = \\ = \sum_{k_s=0}^{N_S-1} r''(1, k_s + i_{seg} N_S) \cdot r''(2, k_s + i_{seg} N_S + n_{\max}) \quad (7)$$

The allowable range of the to be estimated velocity is then bound by

$$v_{\max} = \frac{c}{2} N_s \frac{f_{prf}}{f_s} \ . \quad (8)$$

The velocity resolution is given by

$$v_{\min} = \frac{c}{2} \frac{f_{prf}}{f_s} \ . \quad (9)$$

The estimate of the flow velocity v can be improved by averaging over several pairs of pulses as shown in (10). The position of the correlation peak is determined by arithmetic averaging of j_{max}-1 single peak values where j_{max} is the number of consecutive pulses considered.

$$\hat{R}_d(n_{\max}, i_{seg}) = \\ = \sum_{j=0}^{j_{\max}-2} \sum_{k_s=0}^{N_S-1} r''(j, k_s + i_{seg} N_S) \cdot r''(j+1, k_s + i_{seg} N_S + n_{\max}) \quad (10)$$

By estimating the flow velocity of each $i_{seg} = 0, 1, 2, ..., \left\lfloor \frac{m}{N_s} \right\rfloor$ one obtains $\left\lfloor \frac{m}{N_s} \right\rfloor$ velocity readings for each LOS at different depth locations. The spatially averaged filtered raw data is collected in a 3 dimensional matrix $\boldsymbol{V_z}$ for display.

4. RESULTS

We present a preliminary result of the reconstruction of a 3 dimensional velocity field obtained by isonifying our flow phantom.

To compile the flow voxels 81 slice planes with 81 lines of sight each were interrogated their flow estimated and the result put into a 3 dimensional data structure suitable for MATLABs volume rendering capability. The result of which is shown in Fig. 6 for a single slice plane (k=10 in Fig. 3) and in Fig. 7 for the total data set.

The total computation time for all 81 times 81 LOS with 158 depth pins each on a 1GHz pentium PC was determined to be 3 hours.

The flow velocity profile of the k=10th slice plane shown in Fig. 6 is parabolic and has its maximum at $\hat{v}_z = 0.147$ m/s. The cosine corrected velocity $\hat{v}$ is calculated from the angle θ between the tube and the transducer axis of 65° and the peak flow velocity component $\hat{v}_z$ in the tubing, which results in

$$\hat{v} = \frac{\hat{v}_z}{\cos(\theta)} = 0.348 \text{m/s} \ . \quad (11)$$

If a quadratic flow profile is assumed, this gives an average flow velocity $\bar{\hat{v}}$ of 0.174m/s. The true flow velocity $\bar{v}_{real}$ is know from the pumping speed to be 0.187m/s. The deviation is attributed to the insufficient accuracy of the step motor positioning system.

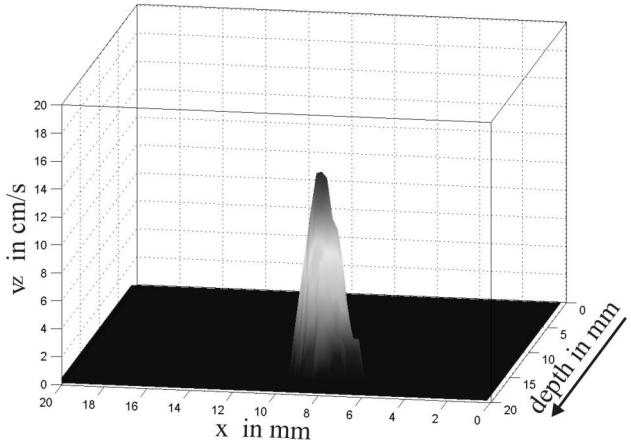

Fig. 6. Results of velocity estimation as applied to a particular slice plane (k=10 as shown in Fig. 3) composed of data from 81 lines of sight (x-dimension)

The velocity data is depicted in a three dimensional plot in Fig. 7 where the scanned volume corresponds to the box in the schematic shown in Fig. 3. The distribution of flow velocity is shown colorcoded in the front slice of the tube.

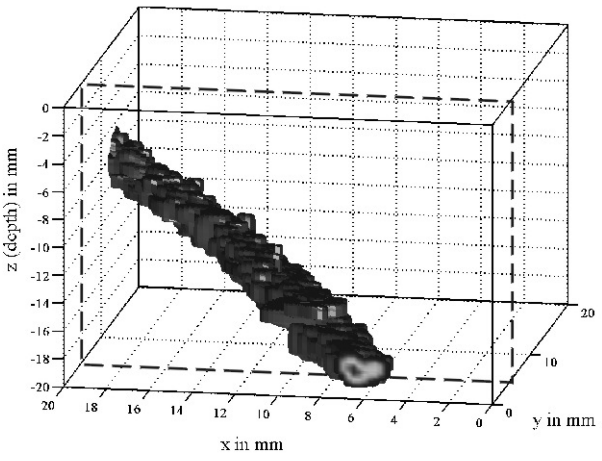

Fig. 7. Result of a 3-dimensional reconstruction of phantom data velocity estimates for 81 slice planes with 81 lines of sight each. An isosurface for v=9mm/s is generated. In the cut-off view of the first slice plane the velocity profile can be seen colorcoded.

5. CONCLUSIONS

As can be seen from the results above fairly nice qualitative as well as quantitative estimates could be achieved by determining the three dimensional velocity distribution in the employed phantom. The deviation of the measured velocity data is most likely due to the rather simple estimator combined with imperfections of the step motor positioning system which will be substituted by a 3D translation stage with a positioning accuracy of better than 10μm. Furthermore the center frequency of the transducer will be increased to 35MHz, which will further increase the spatial resolution. The signal processing algorithm will also be improved.

REFERENCES

[1] J.A. Jensen, "Estimation of Blood Velocities using Ultrasound – a Signal Processing Approach", Cambridge *University Press*, 1996.

[2] K.W. Ferrara, B.G. Zagar, J. Sokil–Melgar, V.R. Algazi, "High Resolution 3D Color Flow Mapping: Applied to the Assessment of Breast Vasculature", Ultrasound in Medicine and Biology, vol. 22, no. 3, pp. 293-304, 1996.

[3] K.W. Ferrara, B.G. Zagar, J.B. Sokil–Melgar, R.H. Silverman, I. M. Aslanidis, "Estimation of Blood Velocity with High Frequency Ultrasound", *IEEE Trans. Ultrasound Freq. Contr.*, vol. 43, no. 1, pp. 149-157, January 1996.

[4] Ch. Kargel, G. Höbenreich, G. Plevnik, B. Trummer, M.F. Insana, "Velocity Estimation and adaptive Clutter Filtering for Color Flow", *Proceedings of WSEAS Multiconference 2002*.

Authors: Florian Maier, Prof. Dr. Bernhard G. Zagar, Institute for Measurement Technology, University of Linz, Altenbergerstrasse 69, 4040 Linz, Austria, +43-70-2468-9208, fax +43-70-2468-9233, florian.maier@jku.at, bernhard.zagar@jku.at .